

# SELF-EVAL: LEVERAGING THE DISCRIMINATIVE NATURE OF GENERATIVE MODELS FOR EVALUATION

Sai Saketh Rambhatla & Ishan Misra

GenAI Meta

{rssaketh, imisra}@meta.com

## ABSTRACT

In this work, we show that text-to-image generative models can be ‘inverted’ to assess their own text-image understanding capabilities in a completely automated manner. Our method, called SELF-EVAL, uses the generative model to compute the likelihood of real images given text prompts, making the generative model directly applicable to discriminative tasks. Using SELF-EVAL, we repurpose standard datasets created for evaluating multimodal text-image discriminative models to evaluate generative models in a fine-grained manner: assessing their performance on attribute binding, color recognition, counting, shape recognition, spatial understanding. To the best of our knowledge SELF-EVAL is the first automated metric to show a high degree of agreement for measuring text-faithfulness with the gold-standard human evaluations across multiple models and benchmarks. Moreover, SELF-EVAL enables us to evaluate generative models on challenging tasks such as Winoground image-score where they demonstrate competitive performance to discriminative models. We also show severe drawbacks of standard automated metrics such as CLIP-score to measure text faithfulness on benchmarks such as DrawBench, and how SELF-EVAL sidesteps these issues. We hope SELF-EVAL enables easy and reliable automated evaluation for diffusion models.

## 1 INTRODUCTION

In the past few years, generative image models have rapidly advanced and state-of-the-art text-to-image models now generate high quality realistic images. While a lot of research effort is focussed on improving these models, their evaluation has received considerably less attention. Evaluations for text-to-image models typically focus on two aspects: (1) quality of the generated image; and (2) the alignment between the generated image and the input text, *i.e.*, the ‘faithfulness’ of the generation. The gold standard for evaluating text-to-image models is to compare generations from pairs of models using human judgement. However, using pairwise human evaluations does not scale to lots of models or generations, and it is an open question on how to convert them to ordinal metrics to rank models. Thus, automatic evaluations are commonly used as a proxy for comparing models.

In this work, we focus on automatic evaluations that measure the ‘text faithfulness’ of the generated image to the input text prompt. While automated evaluations for diffusion models are common, they typically rely on an external discriminative model, *e.g.*, CLIP to measure the ‘relatedness’ of the generated image to the input text. Instead, we ask the question can the diffusion model itself be used to measure the relatedness of an image-text pair and thus evaluate its own generations?

Most work using text-to-image diffusion models focusses on sampling good images from them given a text prompt. However, as shown in Figure 1, diffusion models can be used to estimate the conditional likelihood of an image  $\mathbf{x}$  given a text prompt  $\mathbf{c}$ , *i.e.*,  $p(\mathbf{x}|\mathbf{c})$ . We propose SELF-EVAL which is a practical way to estimate such likelihoods accounting for numerical issues arising in standard diffusion models. We show that these likelihoods can be used directly to evaluate the model’s text-faithfulness. SELF-EVAL repurposes standard multimodal image-text datasets such as Visual Genome, COCO and CLEVR to measure the model’s text understanding capabilities. Our evaluation allows us to assess fine-grained aspects such as the model’s ability to recognize colors, count objects *etc.* We apply our method to a wide variety of diffusion models: different types of image representations (pixel based, latent space based), different text encoders and different model sizes. SELF-EVAL’s automatic evaluation results are in agreement with the ‘gold-standard’ human judgements making SELF-EVAL suitable for evaluation.

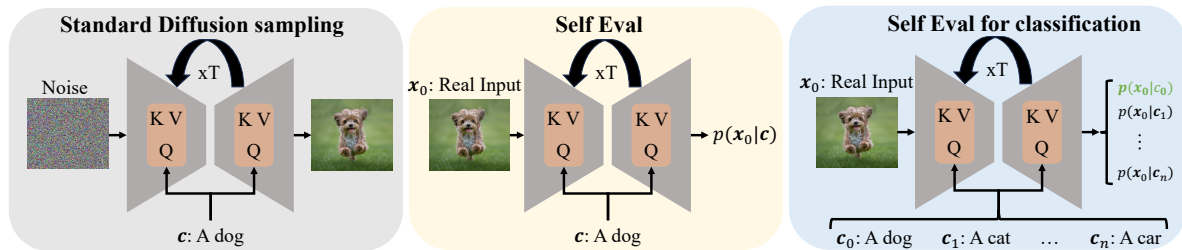


**Figure 1: Illustration of proposed method:** (Left) Starting from a noised input, the standard diffusion sampling method denoises the input iteratively to generate images from the input distribution. (Middle): SELFEVAL takes an image  $\mathbf{x}_0$  and conditioning  $\mathbf{c}$  pairs to estimates the likelihood  $p(\mathbf{x}_0|\mathbf{c})$  of the pair in an iterative fashion. (Right): Given an image,  $\mathbf{x}_0$  and  $n$  captions,  $\{\mathbf{c}_0, \mathbf{c}_1, \dots, \mathbf{c}_n\}$ , SELFEVAL is a principled way to convert generative models into discriminative models. In this work, we show that the classification performance of these classifiers can be used to evaluate the generative capabilities.

SELFEVAL has the added benefit that it does not require additional pretrained models apart from the diffusion models being compared. As we show in Figure 2, relying on an external model leads to three major issues. First, the automated metrics vary greatly depending on the type of the external model used for evaluation. Second, many generative models rely on an external model such as CLIP’s text encoding during training, and thus using the same CLIP model for automated evaluation biases the results. Finally, the external model itself can be bad at certain image-text tasks, such as counting or attribute recognition making its scores unreliable for evaluations.

## 2 RELATED WORKS

**Generative models:** Generative models learn to model the joint distribution,  $p(X, Y)$  of data consisting of an observed variable  $X$  and the target  $Y$ . The model can subsequently be employed to generate novel data through sampling from the learned distribution.. In this work, we are interested in image generation models *i.e.*, models that learn the distribution of natural images. Generative Adversarial Networks (GAN) Goodfellow et al. (2014); Radford et al. (2015), Variational AutoEncoders (VAE) Kingma & Welling (2014) and Denoising Diffusion Probabilistic models (DDPM) Ho et al. (2020) are some of the most popular image generation models in the literature. GANs belong to the category of generative models, where two distinct components, a generator and a discriminator, are pitted against each other within a zero-sum game framework. VAEs are a category of autoencoders that ensure “regularity” within the latent space by constraining their distribution to closely align with a well-behaved and typically standard normal distribution. Subsequently, VQ-VAE’s van den Oord et al. (2017) were proposed to prevent “posterior” collapse that were typically observed with VAEs. In more recent times, DDPMs have exceeded the capabilities of all preceding state-of-the-art image generative models in terms of their generative prowess. Drawing inspiration from non-equilibrium statistical physics, Diffusion probabilistic models Sohl-Dickstein et al. (2015) employ a forward diffusion process to gradually destroy the structure in the unknown input distribution and transforming it into a well-behaved and tractable distribution. A reverse diffusion process is trained to learn to restore the structure, thereby learning the input distribution. Ho et al. (2020) establish an explicit connection between diffusion models and denoising score matching Song & Ermon (2019); Vincent (2011) leading to a simplified objective for training diffusion models. In this study, we employ diffusion models owing to their exceptional image generation performance Dhariwal & Nichol (2021).

**Diffusion models:** In a relatively short time, diffusion models have surpassed GANs and VAEs as the defacto models for image generation due to their superior quality Dhariwal & Nichol (2021) and flexibility. Numerous studies have shown that diffusion models can be conditioned on a variety of modalities, including object classes Peebles & Xie (2023); Ho et al. (2020), natural language captions Saharia et al. (2022); Rombach et al. (2022); Nichol et al. (2022); Ramesh et al. (2022), camera pose Liu et al. (2023), images Brooks et al. (2023), bounding boxes Li et al. (2023b), segmentation, edge and depth maps Zhang & Agrawala (2023). Among these, text-conditioned diffusion models have attracted significant interest and popularity. Given paired image, caption data, the standard way of training text conditioned diffusion models is to fuse the caption features, extracted using a pre-trained text encoder, with the image features while training the reverse diffusion process. The fusion is typically done using cross-attentions Vaswani et al. (2017) layers. Models trained in this manner have demonstrated a remarkable comprehension of compositionality within text, often highlighted by their capac-

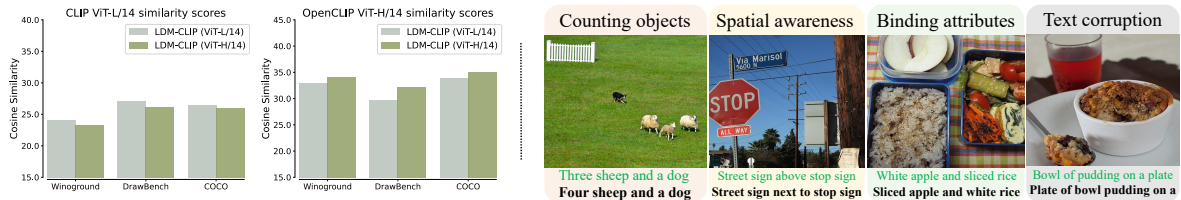


**Figure 2: Drawbacks of CLIP for generative model evaluation.** (Left) We compare the CLIP similarity scores of two Latent diffusion models Rombach et al. (2022) trained with CLIP ViT-L/14 (LDM-CLIP (ViT-L/14)) and OpenCLIP ViT-H/14 (LDM-CLIP (ViT-H/14)) text encoders. On the left, we compare the CLIP similarity scores, computed using CLIP ViT-L/14, on prompts generated from DrawBench, Winoground and, COCO datasets. The plot on the right compares the CLIP similarity scores computed using OpenCLIP ViT-H/14 model. The ranking changes depending on the model used. (Right) CLIP has poor performance in tasks involving counting instances, spatial relationships, matching attributes to objects and understanding corruption of text which constitute about 50 (25%) prompts in DrawBench. In each example, the correct caption is shown in green and CLIP picked the caption in bold. Using CLIP to evaluate text to image models on such prompts is not optimal.

ity to generate images based on counterfactual textual descriptions (like avacado shaped chair *etc.*). The most popular text encoders in use today for text-conditioned image synthesis are text encoders from the CLIP Radford et al. (2021) and the text-to-text transformer T5 Raffel et al. (2020). In this work, we analyze the text understanding capabilities of the diffusion models trained with different text encoders.

There exist two families of diffusion models in the literature, namely, pixel Saharia et al. (2022); Ramesh et al. (2022) and latent diffusion Rombach et al. (2022), differing primarily in the nature of input. As the name suggests, in pixel diffusion, the forward and reverse diffusion processes are performed on the pixels of the input. Performing diffusion on pixels is computationally expensive and hence a typical pixel diffusion pipeline consists of a low resolution generation step followed by a pixel upsampler to get a higher resolution output. Latent diffusion models Rombach et al. (2022) enable training with limited computational budget while simultaneously retaining their quality and flexibility. This is achieved by performing the diffusion process on the latent space of an autoencoder instead of the pixels. In this work, we analyze the text understanding capabilities of two state-of-the-art models with different text encoders each from pixel and latent diffusion models.

**Classifiers with diffusion models:** Lately, there has been a increase in the usage of conditional diffusion models as classifiers, driven by their superior understanding of the conditioned modality. These models are surprisingly good at capturing intricate patterns and dependencies within the conditioning input, making them strong discriminative models across a range of downstream tasks. Notable works include He et al. (2023), Mukhopadhyay et al. (2023) that either finetune a diffusion model, or use linear probing, for several classification and reasoning tasks. Unlike these methods, we do not train any models but instead convert the generative model into a discriminative one to understand its text understanding capabilities. Along similar lines as ours is the work of Clark & Jaini (2023) that observed that the zero-shot performance of the text-to-image pixel diffusion model, Imagen Saharia et al. (2022), is on-par with CLIP Radford et al. (2021) in several downstream tasks. Similar to Clark & Jaini (2023), Li et al. (2023a) adopt the standard ELBO loss as a proxy for the likelihood of a label, given an image, and convert it to a posterior probability using Bayes rule. Authors demonstrate impressive performance on several image classification benchmarks. They also report promising results on ITM tasks on the Winoground Thrush et al. (2022) dataset. We propose a systematic way of estimating the likelihood scores from diffusion models and observe that the performance of generative classifiers, on several Image-Text Matching (ITM) tasks, can be used to evaluate their generative performance. To the best of our knowledge, we are the first method to compare the generative capabilities of different diffusion models using their discriminative performance.

### 3 METHOD: CONVERTING GENERATIVE MODELS TO DISCRIMINATIVE MODELS

Our method converts generative (diffusion) models into discriminative models by simply changing the inference, and does not require any retraining. This allows us to use the diffusion model itself on a variety of different image-text benchmarks and assess the diffusion model’s image-text understanding capabilities. We briefly discuss an overview of diffusion models in Sec. 3.1 followed by our proposed method in Sec. 3.2

### 3.1 PRELIMINARIES

Diffusion Probabilistic Models (DPM) [Sohl-Dickstein et al. \(2015\)](#) are a class of generative models that are trained to ‘denoise’ inputs constructed by a Markovian *forward* process. The forward process starts with a real sample  $\mathbf{x}_0$  and repeatedly adds gaussian noise, over  $t$  timesteps to generate  $\mathbf{x}_t$ :

$$q(\mathbf{x}_t|\mathbf{x}_{t-1}) \sim \mathcal{N}(\mathbf{x}_t; \sqrt{1 - \beta_t}\mathbf{x}_{t-1}, \beta_t\mathbf{I}). \quad (1)$$

Here  $q(\mathbf{x}_0)$  is the data distribution.  $\beta_t$  is the strength of the noise at timestep  $t$  with  $\beta_0 = 0, \beta_T = 1$ . Note that  $\mathbf{x}_t$  are the same size as the input. The joint distribution of the input along with the latents  $q(\mathbf{x}_{0:T})$  is

$$q(\mathbf{x}_{0:T}) = q(\mathbf{x}_0) \prod_{t=1}^T q(\mathbf{x}_t|\mathbf{x}_{t-1}) \quad (2)$$

To sample images, one applies the *reverse* process  $p(\mathbf{x}_{t-1}|\mathbf{x}_t)$ , starting with  $\mathbf{x}_T$  sampled from the unit normal distribution  $\mathcal{N}(\mathbf{0}, \mathbf{I})$ . So the joint distribution of the reverse process can be described as

$$p(\mathbf{x}_{0:T}) = p(\mathbf{x}_T) \prod_{t=1}^T p(\mathbf{x}_{t-1}|\mathbf{x}_t) \quad (3)$$

The reverse process  $p(\mathbf{x}_{t-1}|\mathbf{x}_t)$  is not tractable and is often modeled using a neural network whose parameters are characterized by  $\theta$ , *i.e.*  $p_\theta(\mathbf{x}_{t-1}|\mathbf{x}_t) \sim \mathcal{N}(\mathbf{x}_{t-1}; \boldsymbol{\mu}_\theta(\mathbf{x}_t, t), \boldsymbol{\Sigma}_\theta(\mathbf{x}_t, t))$ .

### 3.2 LIKELIHOOD ESTIMATES FROM DIFFUSION MODELS

We specifically focus on text-to-image diffusion models, although our formulation extends to any conditional diffusion model. Text-to-image diffusion models are trained on a large datasets of image-text  $(\mathbf{x}, \mathbf{c})$  pairs and model the reverse diffusion process  $p(\mathbf{x}_{t-1}|\mathbf{x}_t, \mathbf{c})$ . We ‘invert’ such a generative model and use it to estimate the likelihood of a real image  $\mathbf{x}$  given a text caption  $\mathbf{c}$ , *i.e.*,  $p(\mathbf{x}|\mathbf{c})$ . We note that our method only changes the inference of a diffusion model and does not require any training. Assuming uniform prior on the classes, the likelihood  $p(\mathbf{x}|\mathbf{c})$  can be converted into the posterior,  $p(\mathbf{c}|\mathbf{x})$  using Bayes’ rule, *i.e.*  $p(\mathbf{c}|\mathbf{x}) = \frac{p(\mathbf{x}|\mathbf{c})}{|\mathcal{C}|}$ , where  $\mathcal{C}$  is the set of all classes.

Given the reverse process of a diffusion model parameterized by  $\theta$ , the likelihood for a datapoint  $\mathbf{x}_0$  is

$$p_\theta(\mathbf{x}_0|\mathbf{c}) = \int p_\theta(\mathbf{x}_{0:T}|\mathbf{c}) d\mathbf{x}_{1:T} \quad (4)$$

$$= \int p(\mathbf{x}_T) \prod_{t=1}^T p_\theta(\mathbf{x}_{t-1}|\mathbf{x}_t, \mathbf{c}) d\mathbf{x}_{1:T}. \quad (5)$$

Since the diffusion models reverse process  $p_\theta(\cdot)$  is also a gaussian, we can further write this as

$$p(\mathbf{x}_0|\mathbf{c}) = \int p(\mathbf{x}_T) \prod_{t=1}^T \frac{1}{\sqrt{(2\pi)^D |\boldsymbol{\Sigma}_\theta|}} \exp\left(-\frac{(\mathbf{x}_{t-1} - \boldsymbol{\mu}_\theta(\mathbf{x}_t, \mathbf{c}))^T \boldsymbol{\Sigma}_\theta^{-1} (\mathbf{x}_{t-1} - \boldsymbol{\mu}_\theta(\mathbf{x}_t, \mathbf{c}))}{2}\right) d\mathbf{x}_{1:T} \quad (6)$$

Here,  $p(\mathbf{x}_T) \sim \mathcal{N}(\mathbf{0}, \mathbf{I})$ . For the sake of simplicity, we denote any realization of the random variable  $\mathbf{x}_0$  as  $\mathbf{x}_0$ . Given a natural language caption  $\mathbf{c}$ , an image  $\mathbf{x}_0$  and the noised latents  $\mathbf{x}_{1:T}$ , the quantity inside the integral in Eq. 6 can be estimated numerically. We compute a Monte Carlo estimate of the integral by sampling  $N$  noise terms ( $\epsilon$ ) and computing  $p(\mathbf{x}_0|\mathbf{c})$  as

$$p(\mathbf{x}_0|\mathbf{c}) = \sum_{n=1}^N p(\mathbf{x}_T^n) \prod_{t=1}^T p(\mathbf{x}_{t-1}^n|\mathbf{x}_t^n, \mathbf{c}) \quad \text{where } \mathbf{x}_t^n = \sqrt{1 - \beta_t}\mathbf{x}_{t-1}^n + \sqrt{\beta_t}\epsilon^n \quad (7)$$

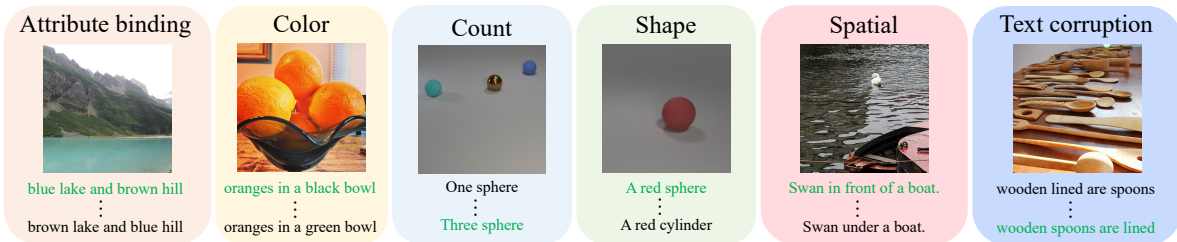


**Figure 3: Representative samples from the benchmark.** We divide the evaluation into six broad tasks, namely `Attribute binding`, `Color`, `Count`, `Shape`, `Spatial`, and `Text corruption`. Each task is designed to evaluate a specific aspect of text faithfulness mimicing the categories in `DrawBench`. Each task is posed as an image-text matching problem, where given an image, the goal is to pick the right caption among distractors. The figure above shows examples from each task with the right caption highlighted in green.

**Practical considerations.** The terms on the RHS of Eq. 7 are multivariate gaussians and analytically computing them involves exponentials which can be numerically unstable. This can be prevented by computing log probabilities instead. Taking log both sides of Eq. 7, we get

$$\log p(\mathbf{x}_0|\mathbf{c}) = \log \sum_{n=1}^N p(\mathbf{x}_T^n) \prod_{t=1}^T p(\mathbf{x}_{t-1}^n|\mathbf{x}_t^n, \mathbf{c}) \quad (8)$$

$$\geq \sum_{n=1}^N (\log p(\mathbf{x}_T^n) + \sum_{t=1}^T \log p(\mathbf{x}_{t-1}^n|\mathbf{x}_t^n, \mathbf{c})) \quad (9)$$

Where the last inequality is due to Jensen’s inequality for concave functions, *i.e.*  $\mathbb{E}(f(x)) \leq f(\mathbb{E}(x))$ . All the terms in Eq. 9 are log probabilities of multivariate gaussians, which can be computed analytically and are numerically more stable.

We now show how estimating  $p(\mathbf{x}_0|\mathbf{c})$  allows us to use a diffusion model for discriminative tasks and thus to evaluate their image-text understanding capabilities.

### 3.3 SELF-EVAL TO EVALUATE DIFFUSION MODEL’S TEXT FAITHFULNESS

The ‘standard’ way of evaluating the text faithfulness of generative models is to 1. manually construct a prompt set that can reason about the model’s capacity to understand the input text, and, 2. evaluate the faithfulness of the generation using human evaluators or an automatic evaluation score, like the CLIP [Radford et al. \(2021\)](#) score. As evaluating the text faithfulness of generative models inherently involves vision-language reasoning, we propose an alternate way to evaluate the model’s performance across discriminative image-text reasoning tasks. In SELF-EVAL, we pose the evaluation as an image-text matching problem and repurpose standard discriminative image-text datasets. Thus, SELF-EVAL does not rely on external models such as CLIP, does not need human evaluators, and does not need manual prompt-set curation.

Image-text matching problems such as image-classification or retrieval can be reformulated as picking the correct caption for a single image  $\mathbf{x}$  from a set of captions  $\{\mathbf{c}_i\}$ . We can use a diffusion model to estimate  $p(\mathbf{x}|\mathbf{c}_i)$  for each of the captions and pick the caption that gives the highest likelihood. As shown in Fig. 1, the noised latents  $\mathbf{x}_{1:T}$  are computed using the forward process. The final latent  $\mathbf{x}_T$  is denoised for  $T$  steps using the reverse process to obtain the denoised latents  $\bar{\mathbf{x}}_{0:T-1}$ . This process is repeated for  $N$  independent noise vectors resulting in  $\{\mathbf{x}_{1:T}^n\}_{n=1}^N$ ,  $\{\bar{\mathbf{x}}_{0:T-1}^n\}_{n=1}^N$ . Next, the likelihood can be computed as  $p(\mathbf{x}_0|\mathbf{c}_k) = \sum_{n=1}^N p(\mathbf{x}_T^n) \prod_{t=1}^T p(\mathbf{x}_{t-1}^n|\bar{\mathbf{x}}_t^n, \mathbf{c}_k)$ , which is then converted to the posterior,  $p(\mathbf{c}_k|\mathbf{x}_0)$  using Bayes’ rule. Finally, the caption with the highest likelihood, *i.e.*  $\arg \max_{\mathbf{c}_i} p(\mathbf{c}_i|\mathbf{x}_0)$  is chosen as the right one.

## 4 EXPERIMENTS

We now use SELF-EVAL to evaluate text-to-image diffusion models. In § 4.1, we introduce our benchmark datasets and models, and present the SELF-EVAL results in § 4.2.

### 4.1 BENCHMARK AND EVALUATION

In SELF-EVAL, we pose the text faithfulness evaluation as an image-text matching problem, where the goal is to pick the right image caption pair among distractors.

**Tasks.** We identify and divide the evaluation into six broad reasoning tasks (illustrated in Figure 3): 1) Attribute binding, 2) Color, 3) Count, 4) Shape, 5) Spatial relationships, and 6) Text corruption. Each of these tasks evaluate the model’s understanding of a specific aspect of text faithfulness and is similar to the categories of prompts from DrawBench Saharia et al. (2022). The six tasks are constructed using data from TIFA Hu et al. (2023), CLEVR Johnson et al. (2016) and ARO Yuksekogunul et al. (2023).

**Datasets.** TIFA Hu et al. (2023) consists of 4000 text prompts, collected manually and from image captioning datasets, to evaluate the text faithfulness of generative models. In our evaluation, we use  $\sim 2000$  of these text-prompts that are constructed from the COCO Lin et al. (2014) dataset and convert the dataset from question-answering to an image-text matching format as detailed in the supplement. **Attribution, Relation and Order (ARO)** Yuksekogunul et al. (2023) is a benchmark that uses data from Visual Genome Krishna et al. (2017) for attribute and spatial relations, and COCO for ordering tasks. **CLEVR** Johnson et al. (2016) is a benchmark for compositional understanding and visual reasoning that uses synthetic images. We use the splits proposed by Lewis et al. (2022) for our experiments.

We divide the datasets among all the reasoning task as follows. For attribute binding, we combine samples from ARO (attribution) and CLEVR. For colors and counts, we use corresponding samples from TIFA and CLEVR. For shapes, use samples from CLEVR. Data for spatial relationships is from TIFA, CLEVR and ARO (relations). The data for the text corruption task is from the ARO (order sensitivity) dataset. A sample of each task consists of an image and multiple text prompts and the performance on the task is the classification accuracy of pairing the image with the right caption.

We measure the performance of text-to-image generative models on the benchmark using the following evaluation methods. We provide full details for each of the methods in the supplement.

**SELF-EVAL (Ours)** is an automatic evaluation method and uses both the images and text from our benchmark introduced in § 4.1. For each benchmark task, we randomly sample 1000 examples and evaluate the classification performance on them. We repeat this three times and the report the mean accuracy. We use 10 trials (*i.e.*  $N = 10$ ) and perform diffusion for 100 steps (*i.e.*  $T = 100$ ) for all the models. Refer to the supplement for ablation experiments on  $N, T$ .

**Human evaluations** are the gold standard for judging the performance of text-to-image models using pairwise comparisons. We present humans with generations from two models and ask them to vote for one of four choices: “both” the generations are faithful, “none” of them are faithful, or if only one of the two images (“Image 1” or “Image 2”) demonstrates fidelity to the given prompt. For simplicity, we only report votes where there is a clear preference for a model. We randomly pick 250 text prompts from each benchmark task as conditioning for human evaluation and the images are generated using DDIM Song et al. (2021) sampling, with 100 denoising steps. Note that unlike SELF-EVAL, human evaluations do *not* use the real images from the benchmark tasks and the human evaluators only look at the generated images.

#### 4.1.1 MODELS

We use models with different image representations: pixel diffusion models which directly use the pixel RGB values, and latent diffusion models where the image is projected into a latent space using an auto-encoder. We pick models trained with different text encoders within each class. This enables us to analyze the effect of text encoder on the final performance within each class.

**Diffusion models with CLIP text encoder.** For latent diffusion, we use a model trained with OpenCLIP Ilharco et al. (2021) text encoder with a ViT-H/14 backbone via an API containing open-sourced model weights. This model is trained on a public dataset with 5 billion images, excluding explicit material, and outputs  $512 \times 512$

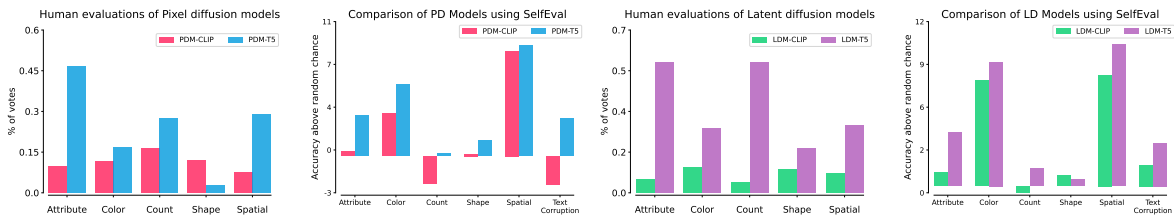


**Figure 4: Evaluating text-to-image models** using human evaluations and SELF-EVAL. We evaluate different types of text-to-image models such as pixel diffusion (first two columns) and latent diffusion model (last two columns), and models that use different text encoders such as T5 XXL and CLIP. We observe that across all 4 diffusion models the relative ordering given by SELF-EVAL’s accuracy correlates with the pairwise human evaluation results. We also observe that latent diffusion models have a higher SELF-EVAL accuracy than pixel diffusion models suggesting better text-faithfulness. Using the stronger T5 text encoder leads to better performance across human evaluations and SELF-EVAL.

images. For pixel diffusion, we adopt the architecture of DALLE-2 [Ramesh et al. \(2022\)](#) for our experiments and train a model. We use a CLIP (ViT-L/14) text encoder and produce images of resolution  $64 \times 64$ . Our model has a total of 4.2B parameters and is trained for 2M steps on an internal image-text dataset (Internal-Dataset).

**Diffusion models with T5 text encoder.** For latent diffusion, we train a UNet model, similar to [Rombach et al. \(2022\)](#), but replace the CLIP text encoder with a T5 XXL [Raffel et al. \(2020\)](#) text encoder that outputs images of resolution  $256 \times 256$ . This model is also trained on Internal-Dataset for 2M steps using a latent space with a  $4\times$  downsampling factor and has a total of 5.8B parameters. We train a 7.5B parameter pixel diffusion model, similar to Imagen [Saharia et al. \(2022\)](#), on inputs of resolution  $64 \times 64$  for 2M steps also on Internal-Dataset. Subsequently, we apply a super resolution model to upsample the output to  $512 \times 512$ .

With the exception of the CLIP-based latent diffusion model [Rombach et al. \(2022\)](#), all the other models are trained for the same number of steps on the exact same data to ensure fair comparison.

## 4.2 MAIN RESULTS

We evaluate the four text-to-image models and report results in Figure 4. For SELF-EVAL, we report the accuracy difference with the random chance accuracy, since each of the tasks has a different degree of difficulty.

**Agreement between SELF-EVAL and human evaluation.** We use both human evaluation and SELF-EVAL to evaluate the four different diffusion models in Figure 4. Human evaluation performance, measured using pairwise comparison, follows the same ranking as given by SELF-EVAL when comparing both types of pixel diffusion models and both types of latent diffusion models. To the best of our knowledge, ours is the first work to establish correlation between the discriminative performance of generative models and human evaluation for text-to-image diffusion models across a wide range of models and tasks. The high degree of alignment between SELF-EVAL and human evaluation suggests that SELF-EVAL is a reliable and interpretable way to evaluate and compare the text faithfulness of different diffusion models.

Next, we use SELF-EVAL to further analyze the performance of diffusion models.

**Effect of the text encoder.** Comparing the different text-encoders used in Figure 4, we observe that diffusion models using the stronger T5 text encoder perform better on most tasks than the ones using the CLIP text encoder. The stronger performance of T5-based models holds for both human evaluations and SELF-EVAL. The SELF-EVAL results also show that diffusion models using the CLIP based encoders have poor performance, worse than random chance, on the Count task. On the Text Corruption task that involves identifying a linguistically correct sentence amongst distractors with a shuffled word order, CLIP-based models show a lower performance. Thus, similar to prior work [Yuksekonul et al. \(2023\)](#), CLIP models show a bag-of-words understanding of the input text and are less sensitive to word order.

**Pixel vs. latent diffusion.** We compare the SELF-EVAL performance of the pixel diffusion models to that of the latent diffusion models in Figure 5. Among models that use the same text encoder, *i.e.* PDM-T5 and LDM-T5, we observe that the latent diffusion models outperform the pixel diffusion ones in most cases, especially on the harder tasks of Attribute Binding, Count, Spatial Relations and Text Corruption. We hypothesize that this difference can be explained by the fact that the latent diffusion models operate on the compressed latent space and prioritize the text conditioning while ‘offloading’ the high-frequency image details

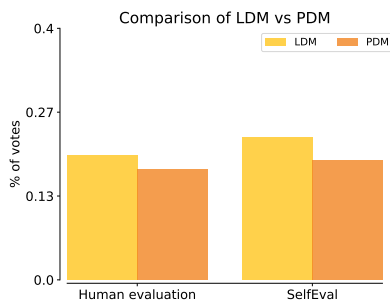


**Figure 5: Pixel vs Latent diffusion.** We observe that human raters rank the generation of latent models higher than pixel models in text faithfulness. We notice a similar ordering using SELF-EVAL.



**Figure 6: Qualitative Results.** (Top): Each example compares the generations of pixel diffusion models with CLIP (left) and T5 (right) text encoders. As the difficulty of the prompt increases, models with stronger text encoders maintain higher text fidelity. Both the models fail on simple prompts from Count and Spatial relationships. (Bottom): Comparison between generations of Pixel (left) and Latent (right) diffusion models with a T5 text encoder. Latent diffusion models can get smaller details like “gray cloth” and “white handles” (second and last example respectively) correctly.

to the autoencoder. We further investigate the performance of pixel and latent diffusion models by employing human raters to evaluate their text faithfulness in Figure 5. The data, for human evaluation, is constructed by randomly picking 500 examples from the all the tasks (100 examples from each task except text corruption), and choosing the right caption as the text prompt. We convert the accuracy of SELF-EVAL, to votes, by counting the number of samples where only one model is right. From Figure 5, we observe that human raters prefer generations of latent diffusion models to pixel diffusion ones for text faithfulness. SELF-EVAL also shows that latent diffusion models have a better text faithfulness and shows an alignment with human evaluations.

**Qualitative results.** Figure 6 (Top) compares the generations of pixel diffusion models that use T5 and CLIP text encoders. In each example, the image on the left and right are generated using CLIP and T5 text encoder respectively. We notice that as the difficulty of prompts increases, models with a stronger text encoder performs better. Both the models fail on the much harder task of counting instances and spatial relationships. In Figure 6 (Bottom), each example consists two images generated using a pixel diffusion model (left) and a latent diffusion model (right) with a T5 text encoder. We observe that unlike the pixel diffusion model, the latent diffusion model can get small yet important details right (“gray table cloth” and “white handles” in the second and sixth example respectively). We believe that the latent diffusion model can offload the high frequency appearance details to the autoencoder, allowing it to pay more attention to the conditioning variable.

#### 4.3 GENERATIVE MODELS APPLIED TO OTHER REASONING TASKS

We now use the challenging Winoground [Thrush et al. \(2022\)](#) benchmark to evaluate the vision-language reasoning abilities of diffusion models. Winoground defines two tasks - (1) ‘text score’ that involves choosing the right text prompt amongst distractors given an input image; and (2) ‘image score’ that involves picking the right image amongst distractor images given a text prompt.

**SELF-EVAL vs. concurrent work** Concurrent work from [Li et al. \(2023a\)](#) demonstrates that diffusion models perform well on the Winoground text score task and achieve competitive performance with discriminative models. Using their formulation yields poor results (zero accuracy) on the image score task as shown in Table 1. [Li et al. \(2023a\)](#) use the ELBO loss as a proxy for the likelihood  $p(\mathbf{x}|\mathbf{c})$  which works well for comparing different text prompts and thus leads to good text score performance. However, our analysis revealed that the ELBO loss computed for the predictions from two different images are not comparable, and thus leads to zero image score. SELF-EVAL on the other hand, doesn’t approximate the likelihood but instead estimates it as described in Sec 3. Using SELF-EVAL leads to a non-zero image-score for the same generative model used by [Li et al. \(2023a\)](#), and yields performance close to that of the discriminative CLIP ViT-L model.

**SELF-EVAL applied to other diffusion models.** Using SELF-EVAL reveals that all the diffusion models introduced in § 4.1.1 achieve competitive performance on both the image score and text score tasks. Compared to all the discriminative CLIP models, generative models achieve strong results in both image and text scores using SELF-EVAL. This result reinforces the notion that optimizing the generative objective can provide non-trivial and complementary improvements for several visuo-linguistic reasoning tasks. For additional analysis on the effect of various hyperparameters on the Winoground performance, refer to the supplement.

**Table 1: Diffusion models evaluated on the Winoground dataset.** We measure the image score (accuracy of picking the correct image given a text prompt) and text score (accuracy of picking the correct text given an image). Using SELFEVAL allows us to use diffusion models for both tasks unlike prior work Li et al. (2023a) which leads to zero image score.

Method	Model	Image Score	Text Score
CLIP (ViT-L/14)	–	8.00	30.25
OCLIP (ViT-H/14)	–	12.75	30.75
Li et al. (2023a)	LDM-CLIP	0	34.00
SELFEVAL	LDM-CLIP	7.25	22.75
SELFEVAL	PDM-CLIP	14.00	17.00
SELFEVAL	PDM-T5	12.00	28.25
SELFEVAL	LDM-T5	13.50	29.00

**Table 2: Performance of CLIP on the benchmark.** We evaluate the zero-shot performance of CLIP (ViT-L/14 visual backbone) on the six tasks. “Random” denotes the random chance accuracy. CLIP achieves impressive performance on the tasks of Color and Shape. We observe that the performance of CLIP is close to random on Attribute binding, Count, Spatial and Text corruption. This makes CLIP unsuitable for evaluating text faithfulness of generative models on prompts from these tasks.

Model	Attribute binding	Color	Count	Shape	Spatial	Text corruption
Random	50	25	25	33	25	20
CLIP	55.40	85.20	67.80	91.10	40.50	51.00

#### 4.4 DRAWBACKS OF CLIP SCORE

In this section, we discuss a few limitations of the CLIP score that SELFEVAL can effectively address. CLIP score is the most common metric for evaluating text faithfulness of generative models by measuring the cosine similarity between the features of the generated image and the conditioned text caption.

##### Sensitivity to the exact CLIP model.

We report the CLIP similarity scores of the generations from two versions of the Latent Diffusion Models Rombach et al. (2022) on prompts from DrawBench Saharia et al. (2022), Winoground Thrush et al. (2022) and COCO-minival Lin et al. (2014) datasets in Figure 2. The first model (LDM-CLIP (ViT-L/14)) uses the text encoder of CLIP with ViT-L/14 backbone and the second model (LDM-CLIP (ViT-H/14)) uses the text encoder with OpenCLIP Ilharco et al. (2021) ViT-H/14 visual backbone. Across all the three datasets, we observe that LDM-CLIP (ViT-L/14) ranks higher than LDM-CLIP (ViT-H/14) if a CLIP (ViT-L/14 visual backbone) model is used, but ranks lower with an OpenCLIP (ViT-H/14 visual backbone). Our hypothesis is that images generated by a model using a particular CLIP text encoder may still contain some residual information, which could cause them to receive higher scores when assessed using the same CLIP model. This type of bias was identified by Park et al. (2021) in the context of evaluation of text-to-image models, though not in relation to the CLIP score. We emphasize the need for caution among researchers who employ this metric, particularly concerning this bias. SELFEVAL avoids this problem as we do not employ an external model for evaluation.

**CLIP score is limited by CLIP’s performance** and thus using it as a proxy on tasks where CLIP itself has poor performance does not yield meaningful comparisons. While the CLIP model has demonstrated impressive zero-shot performance on several image-text tasks, it has severe limitations on many complex reasoning tasks. We compute the performance of CLIP ViT-L/14 model on the six tasks introduced in § 4.1 and report the results in Table 2. CLIP performs well on Color and Shape but its performance on all the other tasks is poor. On the widely used DrawBench prompts, 25% of the captions evaluate the generations for attribute binding, counting, spatial relationships and text corruption. Thus, using CLIP to evaluate generations on such prompts in DrawBench is not ideal. SELFEVAL avoids this problem by directly leveraging the diffusion model itself.

## 5 CONCLUSION

In this paper, we presented SELFEVAL which is an automated way to assess the text-understanding capabilities of diffusion models. Since SELFEVAL uses the diffusion model itself to estimate the likelihood of real images given text prompts, it does not require external discriminative models for such assessments. We showed that evaluations using SELFEVAL agree with human evaluations across a range of models and tasks demonstrating that SELFEVAL is a reliable automated metric. We believe that such metrics can greatly speed up research in diffusion models and further research to improve the metrics is necessary. Since SELFEVAL’s formulation is not limited to text-to-image diffusion models, we believe it can also serve to evaluate other types of conditioned diffusion models such as text-to-audio, text-to-video *etc.* In the future, we want to further generalize SELFEVAL to work with non-diffusion based generative models.

**Acknowledgements:** We are grateful for the support of multiple collaborators at Meta who helped us in this project. We would like to thank Uriel Singer, Adam Polyak, Thomas Hayes, Oron Ashual, Oran Gafni, Sonal Gupta and Yaniv Taigman for their help with training the models. We are grateful to Andrew Brown, Mannat Singh, Quentin Duval, Rohit Girdhar, Samaneh Azadi, Candace Ross for their helpful discussions. We are also grateful to the help from Amy Lee, Payton George, Kelechi Kamanu, Ben Salami and Carolyn Krol. We thank Devi Parikh for her support.

## REFERENCES

- Tim Brooks, Aleksander Holynski, and Alexei A. Efros. Instructpix2pix: Learning to follow image editing instructions. In *CVPR*, 2023. 2
- Kevin Clark and Priyank Jaini. Text-to-image diffusion models are zero-shot classifiers. In *ICLR 2023 Workshop on Multimodal Representation Learning: Perks and Pitfalls*, 2023. URL <https://openreview.net/forum?id=laWYA-LX1Nb>. 3
- Prafulla Dhariwal and Alex Nichol. Diffusion models beat gans on image synthesis. *ArXiv*, abs/2105.05233, 2021. URL <https://api.semanticscholar.org/CorpusID:234357997>. 2
- Ian J. Goodfellow, Jean Pouget-Abadie, Mehdi Mirza, Bing Xu, David Warde-Farley, Sherjil Ozair, Aaron C. Courville, and Yoshua Bengio. Generative adversarial networks. *Communications of the ACM*, 63:139 – 144, 2014. URL <https://api.semanticscholar.org/CorpusID:12209503>. 2
- Xuehai He, Weixi Feng, Tsu-Jui Fu, Varun Jampani, Arjun Akula, Pradyumna Narayana, Sugato Basu, William Yang Wang, and Xin Eric Wang. Discriminative diffusion models as few-shot vision and language learners, 2023. 3
- Jonathan Ho, Ajay Jain, and Pieter Abbeel. Denoising diffusion probabilistic models. In Hugo Larochelle, Marc’Aurelio Ranzato, Raia Hadsell, Maria-Florina Balcan, and Hsuan-Tien Lin (eds.), *Advances in Neural Information Processing Systems 33: Annual Conference on Neural Information Processing Systems 2020, NeurIPS 2020, December 6-12, 2020, virtual*, 2020. URL <https://proceedings.neurips.cc/paper/2020/hash/4c5bcfec8584af0d967flab10179ca4b-Abstract.html>. 2
- Yushi Hu, Benlin Liu, Jungo Kasai, Yizhong Wang, Mari Ostendorf, Ranjay Krishna, and Noah A Smith. Tifa: Accurate and interpretable text-to-image faithfulness evaluation with question answering. *arXiv preprint arXiv:2303.11897*, 2023. 6, 16
- Gabriel Ilharco, Mitchell Wortsman, Ross Wightman, Cade Gordon, Nicholas Carlini, Rohan Taori, Achal Dave, Vaishaal Shankar, Hongseok Namkoong, John Miller, Hannaneh Hajishirzi, Ali Farhadi, and Ludwig Schmidt. Openclip, July 2021. URL <https://doi.org/10.5281/zenodo.5143773>. If you use this software, please cite it as below. 6, 9
- Justin Johnson, Bharath Hariharan, Laurens van der Maaten, Li Fei-Fei, C. Lawrence Zitnick, and Ross B. Girshick. Clevr: A diagnostic dataset for compositional language and elementary visual reasoning. *2017 IEEE Conference on Computer Vision and Pattern Recognition (CVPR)*, pp. 1988–1997, 2016. URL <https://api.semanticscholar.org/CorpusID:15458100>. 6
- Diederik P. Kingma and Max Welling. Auto-encoding variational bayes. In Yoshua Bengio and Yann LeCun (eds.), *2nd International Conference on Learning Representations, ICLR 2014, Banff, AB, Canada, April 14-16, 2014, Conference Track Proceedings*, 2014. URL <http://arxiv.org/abs/1312.6114>. 2
- Ranjay Krishna, Yuke Zhu, Oliver Groth, Justin Johnson, Kenji Hata, Joshua Kravitz, Stephanie Chen, Yannic Kalantidis, Li-Jia Li, David A. Shamma, Michael S. Bernstein, and Li Fei-Fei. Visual genome: Connecting language and vision using crowdsourced dense image annotations. *Int. J. Comput. Vision*, 123(1):32–73, may 2017. ISSN 0920-5691. doi: 10.1007/s11263-016-0981-7. URL <https://doi.org/10.1007/s11263-016-0981-7>. 6
- Martha Lewis, Nihal V. Nayak, Qinan Yu, Jack Merullo, and Elizabeth-Jane Pavlick. Does clip bind concepts? probing compositionality in large image models. *ArXiv*, abs/2212.10537, 2022. URL <https://api.semanticscholar.org/CorpusID:254877746>. 6

- Alexander Cong Li, Mihir Prabhudesai, Shivam Duggal, Ellis Langham Brown, and Deepak Pathak. Your diffusion model is secretly a zero-shot classifier. In *ICML 2023 Workshop on Structured Probabilistic Inference & Generative Modeling*, 2023a. URL <https://openreview.net/forum?id=Ck3yXRdQXD>. 3, 8, 9
- Yuheng Li, Haotian Liu, Qingyang Wu, Fangzhou Mu, Jianwei Yang, Jianfeng Gao, Chunyuan Li, and Yong Jae Lee. Gligen: Open-set grounded text-to-image generation. *2023 IEEE/CVF Conference on Computer Vision and Pattern Recognition (CVPR)*, pp. 22511–22521, 2023b. URL <https://api.semanticscholar.org/CorpusID:255942528>. 2, 15
- Tsung-Yi Lin, Michael Maire, Serge Belongie, James Hays, Pietro Perona, Deva Ramanan, Piotr Dollár, and C. Lawrence Zitnick. Microsoft coco: Common objects in context. In David Fleet, Tomas Pajdla, Bernt Schiele, and Tinne Tuytelaars (eds.), *Computer Vision – ECCV 2014*, pp. 740–755, Cham, 2014. Springer International Publishing. ISBN 978-3-319-10602-1. 6, 9
- Ruoshi Liu, Rundi Wu, Basile Van Hoorick, Pavel Tokmakov, Sergey Zakharov, and Carl Vondrick. Zero-1-to-3: Zero-shot one image to 3d object. *ICCV*, 2023. 2
- Soumik Mukhopadhyay, Matthew Gwilliam, Vatsal Agarwal, Namitha Padmanabhan, Archana Swaminathan, Srinidhi Hegde, Tianyi Zhou, and Abhinav Shrivastava. Diffusion models beat gans on image classification, 2023. 3
- Alexander Quinn Nichol, Prafulla Dhariwal, Aditya Ramesh, Pranav Shyam, Pamela Mishkin, Bob McGrew, Ilya Sutskever, and Mark Chen. GLIDE: towards photorealistic image generation and editing with text-guided diffusion models. In Kamalika Chaudhuri, Stefanie Jegelka, Le Song, Csaba Szepesvári, Gang Niu, and Sivan Sabato (eds.), *International Conference on Machine Learning, ICML 2022, 17-23 July 2022, Baltimore, Maryland, USA*, volume 162 of *Proceedings of Machine Learning Research*, pp. 16784–16804. PMLR, 2022. URL <https://proceedings.mlr.press/v162/nichol22a.html>. 2
- Dong Huk Park, Samaneh Azadi, Xihui Liu, Trevor Darrell, and Anna Rohrbach. Benchmark for compositional text-to-image synthesis. In *Thirty-fifth Conference on Neural Information Processing Systems Datasets and Benchmarks Track (Round 1)*, 2021. URL <https://openreview.net/forum?id=bKBhQhPeKaF>. 9
- William Peebles and Saining Xie. Scalable diffusion models with transformers. *ICCV*, 2023. 2
- Alec Radford, Luke Metz, and Soumith Chintala. Unsupervised representation learning with deep convolutional generative adversarial networks. *CoRR*, abs/1511.06434, 2015. URL <https://api.semanticscholar.org/CorpusID:11758569>. 2
- Alec Radford, Jong Wook Kim, Chris Hallacy, A. Ramesh, Gabriel Goh, Sandhini Agarwal, Girish Sastry, Amanda Askell, Pamela Mishkin, Jack Clark, Gretchen Krueger, and Ilya Sutskever. Learning transferable visual models from natural language supervision. In *ICML*, 2021. 3, 5
- Colin Raffel, Noam Shazeer, Adam Roberts, Katherine Lee, Sharan Narang, Michael Matena, Yanqi Zhou, Wei Li, and Peter J. Liu. Exploring the limits of transfer learning with a unified text-to-text transformer. *Journal of Machine Learning Research*, 21(140):1–67, 2020. URL <http://jmlr.org/papers/v21/20-074.html>. 3, 7
- Aditya Ramesh, Prafulla Dhariwal, Alex Nichol, Casey Chu, and Mark Chen. Hierarchical text-conditional image generation with clip latents, 2022. 2, 3, 7
- Robin Rombach, Andreas Blattmann, Dominik Lorenz, Patrick Esser, and Björn Ommer. High-resolution image synthesis with latent diffusion models. In *Proceedings of the IEEE/CVF Conference on Computer Vision and Pattern Recognition*, pp. 10684–10695, 2022. 2, 3, 7, 9
- Chitwan Saharia, William Chan, Saurabh Saxena, Lala Li, Jay Whang, Emily L. Denton, Seyed Kamyar Seyed Ghasemipour, Burcu Karagol Ayan, Seyedeh Sara Mahdavi, Raphael Gontijo Lopes, Tim Salimans, Jonathan Ho, David J. Fleet, and Mohammad Norouzi. Photorealistic text-to-image diffusion models with deep language understanding. *ArXiv*, abs/2205.11487, 2022. URL <https://api.semanticscholar.org/CorpusID:248986576>. 2, 3, 6, 7, 9

- Jascha Sohl-Dickstein, Eric Weiss, Niru Maheswaranathan, and Surya Ganguli. Deep unsupervised learning using nonequilibrium thermodynamics. In Francis Bach and David Blei (eds.), *Proceedings of the 32nd International Conference on Machine Learning*, volume 37 of *Proceedings of Machine Learning Research*, pp. 2256–2265, Lille, France, 07–09 Jul 2015. PMLR. URL <https://proceedings.mlr.press/v37/sohl-dickstein15.html>. 2, 4
- Jiaming Song, Chenlin Meng, and Stefano Ermon. Denoising diffusion implicit models. In *International Conference on Learning Representations*, 2021. URL <https://openreview.net/forum?id=StlgIarCHLP>. 6
- Yang Song and Stefano Ermon. Generative modeling by estimating gradients of the data distribution. In H. Wallach, H. Larochelle, A. Beygelzimer, F. d'Alché-Buc, E. Fox, and R. Garnett (eds.), *Advances in Neural Information Processing Systems*, volume 32. Curran Associates, Inc., 2019. URL [https://proceedings.neurips.cc/paper\\_files/paper/2019/file/3001ef257407d5a371a96dcd947c7d93-Paper.pdf](https://proceedings.neurips.cc/paper_files/paper/2019/file/3001ef257407d5a371a96dcd947c7d93-Paper.pdf). 2
- Tristan Thrush, Ryan Jiang, Max Bartolo, Amanpreet Singh, Adina Williams, Douwe Kiela, and Candace Ross. Winoground: Probing vision and language models for visio-linguistic compositionality. *2022 IEEE/CVF Conference on Computer Vision and Pattern Recognition (CVPR)*, pp. 5228–5238, 2022. URL <https://api.semanticscholar.org/CorpusID:248006414>. 3, 8, 9, 15
- Aaron van den Oord, Oriol Vinyals, and koray kavukcuoglu. Neural discrete representation learning. In I. Guyon, U. Von Luxburg, S. Bengio, H. Wallach, R. Fergus, S. Vishwanathan, and R. Garnett (eds.), *Advances in Neural Information Processing Systems*, volume 30. Curran Associates, Inc., 2017. URL [https://proceedings.neurips.cc/paper\\_files/paper/2017/file/7a98af17e63a0ac09ce2e96d03992fbc-Paper.pdf](https://proceedings.neurips.cc/paper_files/paper/2017/file/7a98af17e63a0ac09ce2e96d03992fbc-Paper.pdf). 2
- Ashish Vaswani, Noam Shazeer, Niki Parmar, Jakob Uszkoreit, Llion Jones, Aidan N Gomez, Łukasz Kaiser, and Illia Polosukhin. Attention is all you need. In I. Guyon, U. Von Luxburg, S. Bengio, H. Wallach, R. Fergus, S. Vishwanathan, and R. Garnett (eds.), *Advances in Neural Information Processing Systems*, volume 30. Curran Associates, Inc., 2017. URL [https://proceedings.neurips.cc/paper\\_files/paper/2017/file/3f5ee243547dee91fbd053c1c4a845aa-Paper.pdf](https://proceedings.neurips.cc/paper_files/paper/2017/file/3f5ee243547dee91fbd053c1c4a845aa-Paper.pdf). 2
- Pascal Vincent. A connection between score matching and denoising autoencoders. *Neural Computation*, 23(7):1661–1674, 2011. doi: 10.1162/NECO\_a.00142. 2
- Mert Yuksekgonul, Federico Bianchi, Pratyusha Kalluri, Dan Jurafsky, and James Zou. When and why vision-language models behave like bags-of-words, and what to do about it? In *International Conference on Learning Representations*, 2023. URL <https://openreview.net/forum?id=KRLUvxh8uaX>. 6, 7
- Lvmin Zhang and Maneesh Agrawala. Adding conditional control to text-to-image diffusion models, 2023. 2

## A ADDITIONAL DETAILS OF SELFEVAL

In this section, we provide a detailed algorithm and systematic figure of SELFEVAL in Algorithm 1 and Figure 7 respectively. SELFEVAL iteratively denoises an image, similar to the reverse process of diffusion models, but instead estimates the likelihood of an image-text pair.

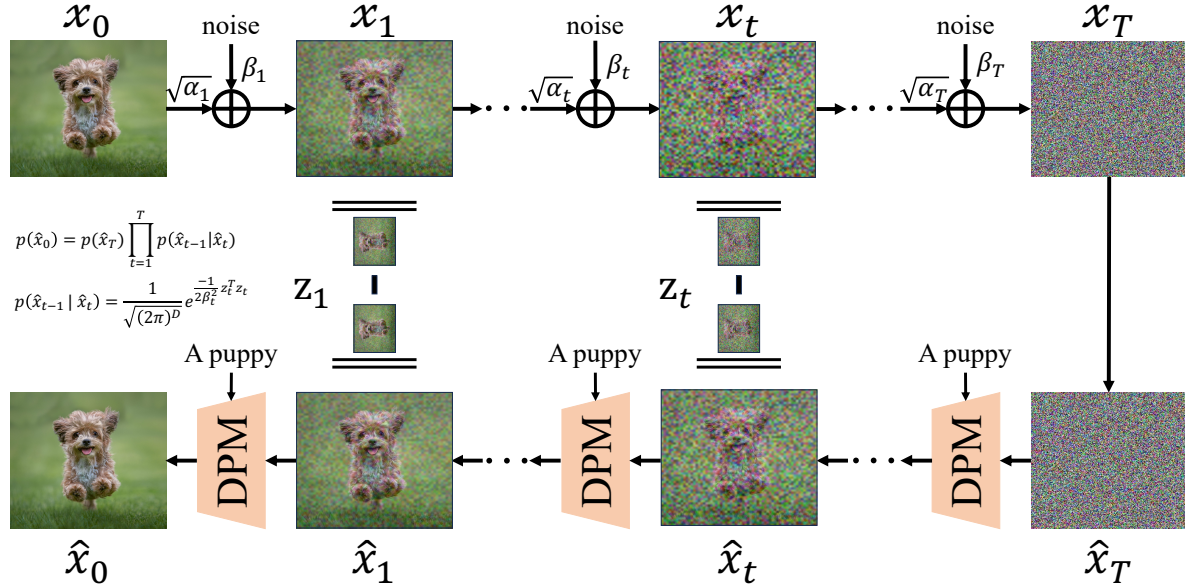


**Figure 7: Illustration of proposed method:** (Left) Starting from a noised input, the standard diffusion sampling method denoises the input iteratively to generate images from the input distribution. (Middle): SelfEval takes an image  $x_0$  and conditioning  $c$  pairs to estimate the likelihood  $p(x_0|c)$  of the pair in an iterative fashion. (Right): Given an image,  $x_0$  and  $n$  captions,  $\{c_0, c_1, \dots, c_n\}$ , SelfEval is a principled way to convert generative models into discriminative models. In this work, we show that the classification performance of these classifiers can be used to evaluate the generative capabilities.

---

### Algorithm 1 Algorithm for estimating $p(\mathbf{x}|\mathbf{c})$ using SELFEVAL

---

- 1: **Input:** Diffusion model  $p_\theta(\mathbf{x}_{t-1}|\mathbf{x}_t)$ ; Input image  $\mathbf{x}_0$ ; Forward latents:  $\{\mathbf{x}_{1:T}\}$ ; Reverse latents:  $\{\hat{\mathbf{x}}_{1:T}\}$ ; Number of trials:  $N$
  - 2: **for**  $i=1:N$  **do**
  - 3:   Sample noise  $\sim \mathcal{N}(0, \mathbb{I})$
  - 4:    $\mathbf{x}_{1:T} = q_{\text{sample}}(\mathbf{x}_0, t = 1 : T, \text{noise} = \text{noise}); \mathbf{x}_t \in \mathbb{R}^D$
  - 5:   conditionals  $\leftarrow [ ]$
  - 6:   **for**  $j=1:T$  **do**
  - 7:      $p(\mathbf{x}_{t-1}|\bar{\mathbf{x}}_t, \mathbf{c}) = \frac{1}{\sqrt{(2\pi)^D |\Sigma_\theta|}} e^{-0.5(\mathbf{x}_{t-1} - \mu_\theta(\bar{\mathbf{x}}_t, t, \mathbf{c}))^T \Sigma_\theta^{-1} (\mathbf{x}_{t-1} - \mu_\theta(\bar{\mathbf{x}}_t, t, \mathbf{c}))}$
  - 8:     conditionals = [conditionals ;  $p(\mathbf{x}_{t-1}|\bar{\mathbf{x}}_t, \mathbf{c})$ ]
  - 9:   **end for**
  - 10:   Compute  $p(\mathbf{x}_T) = \frac{1}{\sqrt{(2\pi)^D}} e^{-\frac{1}{2\beta_T^2} \|\mathbf{x}_T\|^2}$
  - 11:   Compute likelihood  $p_i(\mathbf{x}_0|\mathbf{c}) = p(\mathbf{x}_T) \prod_{t=1}^T p(\mathbf{x}_{t-1}|\bar{\mathbf{x}}_t, \mathbf{c})$
  - 12: **end for**
  - 13:  $p(\mathbf{c}|\mathbf{x}_0) = \frac{p(\mathbf{x}_0|\mathbf{c})}{|\mathbf{c}|}$
-

## B DETAILS OF HUMAN EVALUATION

Human evaluations are the de-facto standard for judging the performance of text-to-image models. we adopt a conventional A/B testing approach, wherein raters are presented with generations from two models and are asked to vote for one of four choices: “both” the generations are faithful, “none” of them are faithful, or if only one of the two models (“model 1” or “model 2”) demonstrates fidelity to the given prompt. We show the template provided to the raters in Figure 8. The template includes three examples that advice the raters on how to rate a given sample followed by a text prompt and two images. The four possible choices are shown on the right in Figure 9. The images used as instructions for the human raters are shown in Figure 9. Figure 9 shows three pairs of images with the text prompt below them. The first example shows two images that are faithful to the input prompt but the quality of one (left) image superior to the other (right). Since, we ask the raters to evaluate the text faithfulness, we recommend picking the “both” option for such samples. The second image shows an example where only one of the images is faithful to the text. The raters are instructed to pick the option corresponding to the right image in this case. The final example shows two images that are not faithful to the text prompt. The raters are advised to pick the “none” option in this scenario.

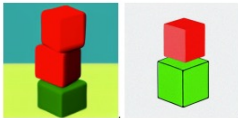
Please read all the instructions carefully before answering the questions



Consider a text "A brown bear and a blue bird" and the two images . In this example, note that image on the left is of higher quality than the one on the right, but **both** the images are well aligned with the text. So the right answer to pick is "Both".

=====

Consider a text "A stack of 3 cubes. A red cube is on the top, sitting on a red cube. The red cube is in the middle, sitting on a green cube. The green cube is on the bottom".



Given the two images , the image on the left aligns well with the text while the image on the right misses it. So the right answer should be "Image 1".

=====



Consider the text "A herd of sheep chased by a border collie" and two images . Both the images have a "small herd of sheep" but no "border collie". In this case, the correct answer is "None". Note that even if an image is **not aligned with a small portion of the text**, it should **not** be picked as the right answer.

=====

**Text:** A purple cylinder and a red cube

Image 1



Image 2



Select an option

None	1
Image 1	2
Image 2	3
Both	4

**Figure 8: Template for Human raters.** The template consists of instructions explaining the nature of the task (top) followed by a text prompt with two generations (bottom). Humans are expected to pick one of four options (shown on the right): “both” the generations are faithful, “none” of them are faithful, or if only one of the two images (“Image 1” or “Image 2”) demonstrates fidelity to the text prompt.

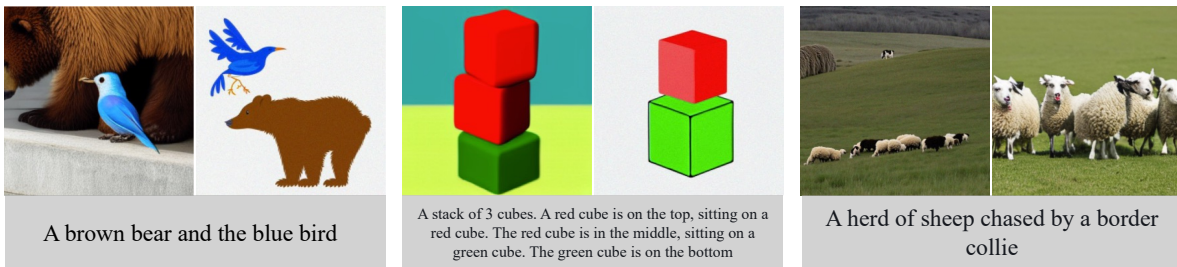


**Figure 9: Instructions for Human raters.** We provide three examples describing all the possible scenarios. The first example shows two images that are faithful to the text but with varying image qualities. To prevent the raters from conflating image quality with text faithfulness, we recommend the raters to pick “both” for such examples. The second example illustrates a case where only one of the image is faithful to the text. In this case, the raters are advised to pick the option corresponding to the right image (“Image 1” in this case). The final example shows a case where both the examples are not faithful to the text (there is no border collie), in which case, we advice the raters to pick “none”.

## C ABLATION EXPERIMENTS

**Table 3: Effect of timesteps** on the performance of SELF-EVAL on the six splits.

T	Attribute	Color	Count	Shape	Spatial	Text Corruption
50	54.2	32.2	26.3	34.9	33.0	25
100	54.3	34	25.8	30.2	38.0	24.3
250	53	32.3	27.4	35	32.7	21.7

**Table 4: Effect of N** on the performance of SELF-EVAL on the six splits.

N	Attribute	Color	Count	Shape	Spatial	Text Corruption
1	53.0	26.0	27.2	35.2	31.2	20.7
5	54.3	31.7	25.7	34.9	33.0	22.1
10	54.3	34.0	25.8	32.5	38.6	24.3
15	53.4	36.3	28.0	36.3	32.8	22.8

**Table 5: Effect of the choice of seed** on the performance of SELF-EVAL.

S	Attribute	Color	Count	Shape	Spatial	Text Corruption
1	54.3	34.0	25.8	32.5	38.6	24.3
2	53.0	26.0	27.2	35.2	31.2	20.7
3	54.3	31.70	25.7	34.9	33.0	22.1
std	0.5	0.5	0.9	1.4	1.5	0.8

In this section we analyze the effect of various components that affect the performance of SELF-EVAL on the six splits introduced in the main paper. We use the LDM-T5 model for all our experiments.

**Effect of T:** SELF-EVAL has a time complexity of  $\mathcal{O}(NT)$  and Table 3 shows the the effect of timesteps on the performance of SELF-EVAL. We observe that SELF-EVAL achieves the best result at different timesteps for different datasets. We notice that the performance drops as we increase the timesteps from 100 to 250 in most cases. As the number of timesteps increases, we believe that the fraction of them responsible for text faithfulness decrease, resulting in a drop in performance. We find  $T = 100$  to be a good tradeoff for performance and speed and is used for all the experiments on the six data splits in this work.

**Effect of N:** Table 4 shows the results of the effect of number of trials  $N$  on the performance of SELF-EVAL. We observe that  $N = 10$  works best across all the six splits and is the default choice for  $N$  unless otherwise mentioned.

**Effect of seeds:** SELF-EVAL corrupts an input image using standard gaussian noise in each trial and we analyze the effect of the seed on the performance of SELF-EVAL in Table 5. We observe that the performance is stable across all the six splits with a standard deviation within 1 percentage point in most of the cases. We report the seed number instead of the actual value for brevity and use the seed 1 as the default choice for all the experiments.

## D ADDITIONAL EXPERIMENTS ON WINOGROUND

In this section we ablate a few design decisions on the Winoground dataset. We use the LDM-T5 model for all the experiments.

**Effect of T:** We show the effect of the number of timesteps on the performance of SELF-EVAL on the Winoground dataset in Table 6. From Table 6, we observe that SELF-EVAL achieves the best result for image and text score at different time steps. Image score is a harder task compared to Text score [Thrush et al. \(2022\)](#) and hence SELF-EVAL needs more timesteps to perform better on Image score. As the number of timesteps increase, we observe a drop in both Image and Text scores. Studies [Li et al. \(2023b\)](#) show that the earlier timesteps generate low frequency information (responsible for text fidelity), while latter ones are responsible for high frequency

**Table 6: Effect of timesteps** on **Table 7: Effect of the number of trials** on the performance of SELFEVAL on the Winoground dataset **Table 8: Effect of the choice of seed** on the performance of SELFEVAL on the Winoground dataset

T	Image Score	Text Score	N	Image Score	Text Score	S	Image Score	Text Score
20	11.50	30.75	1	17.00	26.25	1	13.50	29.00
50	13.50	29.00	5	14.75	26.00	2	13.00	27.00
100	12.25	25.25	10	13.50	29.00	3	12.00	28.50
250	11.25	27.75	20	11.25	24.75		12.83± 0.76	28.17±1.04

appearance details. By increasing the number of timesteps, the fraction of timesteps contributing to improving the faithfulness to text (and thereby image and text scores) decreases, resulting in a drop in performance. All other experiments on Winoground use T=50 unless otherwise specified.

**Effect of N:** We show the effect of the number of trials (N) in Table 7. With fewer trials, the estimates are not reliable and larger trials make it computationally expensive. We observe that we attain a good tradeoff for performance and speed with  $N = 10$ .

**Effect of the seed:** We show the effect of seed on the performance of SELFEVAL in Table 8. We just report the seed number for brevity. We observe that both the scores are relatively stable across different values of seed. We fix seed #1 for all the experiments in this work.

## E CONVERTING COCO IMAGE-CAPTION PAIRS FOR ITM

We use image-caption pairs from COCO for the tasks of `Color`, `Count` and `Spatial relationships`. We use the question answering data collected by authors of TIFA [Hu et al. \(2023\)](#) to construct data for our tasks. We pick only samples constructed from COCO for our purpose. Given question answering samples from TIFA, we identify the corresponding image-caption pair from COCO and replace the correct answer in the caption with the multiple choices to form samples for the task of Image-Text Matching.

# SELF<sub>E</sub>VAL: LEVERAGING THE DISCRIMINATIVE NATURE OF GENERATIVE MODELS FOR EVALUATION

arXiv:2311.10708v1 [cs.CV] 17 Nov 2023

## A ADDITIONAL DETAILS OF SELFEVAL

In this section, we provide a detailed algorithm and systematic figure of SELFEVAL in Algorithm 1 and Figure 1 respectively. SELFEVAL iteratively denoises an image, similar to the reverse process of diffusion models, but instead estimates the likelihood of an image-text pair.

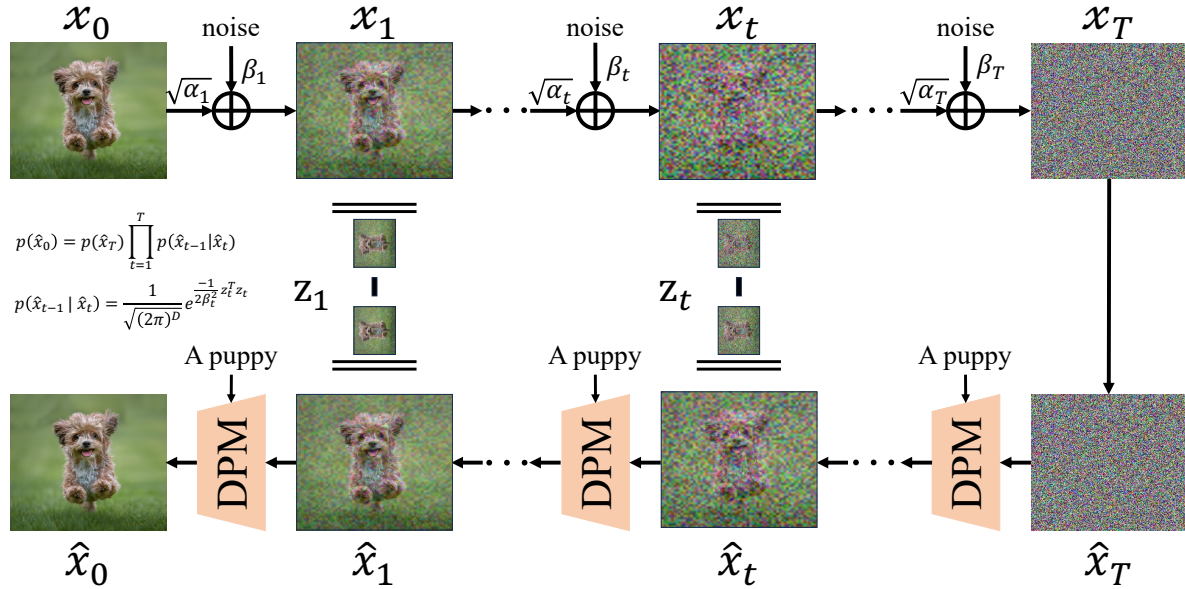


**Figure 1: Illustration of proposed method:** (Left) Starting from a noised input, the standard diffusion sampling method denoises the input iteratively to generate images from the input distribution. (Middle): SelfEval takes an image  $x_0$  and conditioning  $c$  pairs to estimate the likelihood  $p(x_0|c)$  of the pair in an iterative fashion. (Right): Given an image,  $x_0$  and  $n$  captions,  $\{c_0, c_1, \dots, c_n\}$ , SelfEval is a principled way to convert generative models into discriminative models. In this work, we show that the classification performance of these classifiers can be used to evaluate the generative capabilities.

---

### Algorithm 1 Algorithm for estimating $p(\mathbf{x}|\mathbf{c})$ using SELFEVAL

---

- 1: **Input:** Diffusion model  $p_\theta(\mathbf{x}_{t-1}|\mathbf{x}_t)$ ; Input image  $\mathbf{x}_0$ ; Forward latents:  $\{\mathbf{x}_{1:T}\}$ ; Reverse latents:  $\{\hat{\mathbf{x}}_{1:T}\}$ ; Number of trials:  $N$
  - 2: **for**  $i=1:N$  **do**
  - 3:   Sample noise  $\sim \mathcal{N}(0, \mathbb{I})$
  - 4:    $\mathbf{x}_{1:T} = q_{\text{sample}}(\mathbf{x}_0, t = 1 : T, \text{noise} = \text{noise}); \mathbf{x}_t \in \mathbb{R}^D$
  - 5:   conditionals  $\leftarrow [ ]$
  - 6:   **for**  $j=1:T$  **do**
  - 7:      $p(\mathbf{x}_{t-1}|\bar{\mathbf{x}}_t, \mathbf{c}) = \frac{1}{\sqrt{(2\pi)^D |\Sigma_\theta|}} e^{-0.5(\mathbf{x}_{t-1} - \mu_\theta(\bar{\mathbf{x}}_t, t, \mathbf{c}))^T \Sigma_\theta^{-1} (\mathbf{x}_{t-1} - \mu_\theta(\bar{\mathbf{x}}_t, t, \mathbf{c}))}$
  - 8:     conditionals = [conditionals ;  $p(\mathbf{x}_{t-1}|\bar{\mathbf{x}}_t, \mathbf{c})$ ]
  - 9:   **end for**
  - 10:   Compute  $p(\mathbf{x}_T) = \frac{1}{\sqrt{(2\pi)^D}} e^{-\frac{1}{2\beta_T^2} \|\mathbf{x}_T\|^2}$
  - 11:   Compute likelihood  $p_i(\mathbf{x}_0|\mathbf{c}) = p(\mathbf{x}_T) \prod_{t=1}^T p(\mathbf{x}_{t-1}|\bar{\mathbf{x}}_t, \mathbf{c})$
  - 12: **end for**
  - 13:  $p(\mathbf{c}|\mathbf{x}_0) = \frac{p(\mathbf{x}_0|\mathbf{c})}{|\mathbf{c}|}$
-

### B DETAILS OF HUMAN EVALUATION

Human evaluations are the de-facto standard for judging the performance of text-to-image models. we adopt a conventional A/B testing approach, wherein raters are presented with generations from two models and are asked to vote for one of four choices: “both” the generations are faithful, “none” of them are faithful, or if only one of the two models (“model 1” or “model 2”) demonstrates fidelity to the given prompt. We show the template provided to the raters in Figure 2. The template includes three examples that advice the raters on how to rate a given sample followed by a text prompt and two images. The four possible choices are shown on the right in Figure 3. The images used as instructions for the human raters are shown in Figure 3. Figure 3 shows three pairs of images with the text prompt below them. The first example shows two images that are faithful to the input prompt but the quality of one (left) image superior to the other (right). Since, we ask the raters to evaluate the text faithfulness, we recommend picking the “both” option for such samples. The second image shows an example where only one of the images is faithful to the text. The raters are instructed to pick the option corresponding to the right image in this case. The final example shows two images that are not faithful to the text prompt. The raters are advised to pick the “none” option in this scenario.

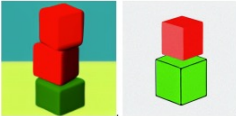
Please read all the instructions carefully before answering the questions



Consider a text "A brown bear and a blue bird" and the two images. In this example, note that image on the left is of higher quality than the one on the right, but **both** the images are well aligned with the text. So the right answer to pick is "Both".

=====

Consider a text "A stack of 3 cubes. A red cube is on the top, sitting on a red cube. The red cube is in the middle, sitting on a green cube. The green cube is on the bottom".



Given the two images, the image on the left aligns well with the text while the image on the right misses it. So the right answer should be "Image 1".

=====



Consider the text "A herd of sheep chased by a border collie" and two images. Both the images have a "small herd of sheep" but no "border collie". In this case, the correct answer is "None". Note that even if an image is **not aligned with a small portion of the text**, it should **not** be picked as the right answer.

=====

**Text:** A purple cylinder and a red cube

Image 1



Image 2



Select an option

None	1
Image 1	2
Image 2	3
Both	4

**Figure 2: Template for Human raters.** The template consists of instructions explaining the nature of the task (top) followed by a text prompt with two generations (bottom). Humans are expected to pick one of four options (shown on the right): “both” the generations are faithful, “none” of them are faithful, or if only one of the two images (“Image 1” or “Image 2”) demonstrates fidelity to the text prompt.

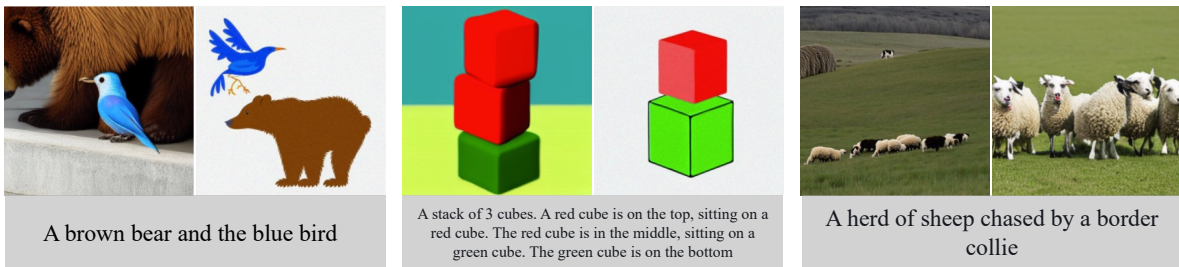


**Figure 3: Instructions for Human raters.** We provide three examples describing all the possible scenarios. The first example shows two images that are faithful to the text but with varying image qualities. To prevent the raters from conflating image quality with text faithfulness, we recommend the raters to pick “both” for such examples. The second example illustrates a case where only one of the image is faithful to the text. In this case, the raters are advised to pick the option corresponding to the right image (“Image 1” in this case). The final example shows a case where both the examples are not faithful to the text (there is no border collie), in which case, we advice the raters to pick “none”.

## C ABLATION EXPERIMENTS

**Table 1: Effect of timesteps** on the performance of SELF-EVAL on the six splits.

T	Attribute	Color	Count	Shape	Spatial	Text Corruption
50	54.2	32.2	26.3	34.9	33.0	25
100	54.3	34	25.8	30.2	38.0	24.3
250	53	32.3	27.4	35	32.7	21.7

**Table 2: Effect of N** on the performance of SELF-EVAL on the six splits.

N	Attribute	Color	Count	Shape	Spatial	Text Corruption
1	53.0	26.0	27.2	35.2	31.2	20.7
5	54.3	31.7	25.7	34.9	33.0	22.1
10	54.3	34.0	25.8	32.5	38.6	24.3
15	53.4	36.3	28.0	36.3	32.8	22.8

**Table 3: Effect of the choice of seed** on the performance of SELF-EVAL.

S	Attribute	Color	Count	Shape	Spatial	Text Corruption
1	54.3	34.0	25.8	32.5	38.6	24.3
2	53.0	26.0	27.2	35.2	31.2	20.7
3	54.3	31.70	25.7	34.9	33.0	22.1
std	0.5	0.5	0.9	1.4	1.5	0.8

In this section we analyze the effect of various components that affect the performance of SELF-EVAL on the six splits introduced in the main paper. We use the LDM-T5 model for all our experiments.

**Effect of T:** SELF-EVAL has a time complexity of  $\mathcal{O}(NT)$  and Table 1 shows the the effect of timesteps on the performance of SELF-EVAL. We observe that SELF-EVAL achieves the best result at different timesteps for different datasets. We notice that the performance drops as we increase the timesteps from 100 to 250 in most cases. As the number of timesteps increases, we believe that the fraction of them responsible for text faithfulness decrease, resulting in a drop in performance. We find  $T = 100$  to be a good tradeoff for performance and speed and is used for all the experiments on the six data splits in this work.

**Effect of N:** Table 2 shows the results of the effect of number of trials  $N$  on the performance of SELF-EVAL. We observe that  $N = 10$  works best across all the six splits and is the default choice for  $N$  unless otherwise mentioned.

**Effect of seeds:** SELF-EVAL corrupts an input image using standard gaussian noise in each trial and we analyze the effect of the seed on the performance of SELF-EVAL in Table 3. We observe that the performance is stable across all the six splits with a standard deviation within 1 percentage point in most of the cases. We report the seed number instead of the actual value for brevity and use the seed 1 as the default choice for all the experiments.

## D ADDITIONAL EXPERIMENTS ON WINOGROUND

In this section we ablate a few design decisions on the Winoground dataset. We use the LDM-T5 model for all the experiments.

**Effect of T:** We show the effect of the number of timesteps on the performance of SELF-EVAL on the Winoground dataset in Table 4. From Table 4, we observe that SELF-EVAL achieves the best result for image and text score at different time steps. Image score is a harder task compared to Text score [Thrush et al. \(2022\)](#) and hence SELF-EVAL needs more timesteps to perform better on Image score. As the number of timesteps increase, we observe a drop in both Image and Text scores. Studies [Li et al. \(2023\)](#) show that the earlier timesteps generate low frequency information (responsible for text fidelity), while latter ones are responsible for high frequency

**Table 4: Effect of timesteps** on the performance of SELFEVAL on the Winoground dataset  
**Table 5: Effect of the number of trials** on the performance of SELFEVAL on the Winoground dataset  
**Table 6: Effect of the choice of seed** on the performance of SELFEVAL on the Winoground dataset

T	Image Score	Text Score	N	Image Score	Text Score	S	Image Score	Text Score
20	11.50	30.75	1	17.00	26.25	1	13.50	29.00
50	13.50	29.00	5	14.75	26.00	2	13.00	27.00
100	12.25	25.25	10	13.50	29.00	3	12.00	28.50
250	11.25	27.75	20	11.25	24.75		12.83± 0.76	28.17±1.04

appearance details. By increasing the number of timesteps, the fraction of timesteps contributing to improving the faithfulness to text (and thereby image and text scores) decreases, resulting in a drop in performance. All other experiments on Winoground use T=50 unless otherwise specified.

**Effect of N:** We show the effect of the number of trials (N) in Table 5. With fewer trials, the estimates are not reliable and larger trials make it computationally expensive. We observe that we attain a good tradeoff for performance and speed with  $N = 10$ .

**Effect of the seed:** We show the effect of seed on the performance of SELFEVAL in Table 6. We just report the seed number for brevity. We observe that both the scores are relatively stable across different values of seed. We fix seed #1 for all the experiments in this work.

## E CONVERTING COCO IMAGE-CAPTION PAIRS FOR ITM

We use image-caption pairs from COCO for the tasks of `Color`, `Count` and `Spatial relationships`. We use the question answering data collected by authors of TIFA Hu et al. (2023) to construct data for our tasks. We pick only samples constructed from COCO for our purpose. Given question answering samples from TIFA, we identify the corresponding image-caption pair from COCO and replace the correct answer in the caption with the multiple choices to form samples for the task of Image-Text Matching.

## REFERENCES

- Yushi Hu, Benlin Liu, Jungo Kasai, Yizhong Wang, Mari Ostendorf, Ranjay Krishna, and Noah A Smith. Tifa: Accurate and interpretable text-to-image faithfulness evaluation with question answering. *arXiv preprint arXiv:2303.11897*, 2023. 5
- Yuheng Li, Haotian Liu, Qingyang Wu, Fangzhou Mu, Jianwei Yang, Jianfeng Gao, Chunyuan Li, and Yong Jae Lee. Gligen: Open-set grounded text-to-image generation. *2023 IEEE/CVF Conference on Computer Vision and Pattern Recognition (CVPR)*, pp. 22511–22521, 2023. URL <https://api.semanticscholar.org/CorpusID:255942528>. 4
- Tristan Thrush, Ryan Jiang, Max Bartolo, Amanpreet Singh, Adina Williams, Douwe Kiela, and Candace Ross. Winoground: Probing vision and language models for visio-linguistic compositionality. *2022 IEEE/CVF Conference on Computer Vision and Pattern Recognition (CVPR)*, pp. 5228–5238, 2022. URL <https://api.semanticscholar.org/CorpusID:248006414>. 4